Project Acronym: Nutrishield
Grant Agreement number: 818110 (H2020-SFS-2018-IA)
Project Full Title: Fact-based personalised nutrition for the young

DELIVERABLE

D4.1 – Report on chemical analysis methods & Suggested spectroscopic parameters for detection

Dissemination level	PU - public
Type of Document	Report
Contractual date of delivery	31/10/2019
Deliverable Leader	TU Wien (TUW)
Status & version	V2.0– 10/23/2019
WP responsible	QRT (WP4 leader)
Keywords:	Urine analysis, human milk analysis, breath analysis, phosphate, creatinine, protein, casein, lactoferrin, α-lactalbumin, methane, hydrogen cyanide

Deliverable Leader:	TUW
Contributors:	ARGOS, RU, HULAFE, CSEM, QRT
Reviewers:	TUW, ARGOS, CSEM, QRT, ALPES, INTRA
Approved by:	ALPES, INTRA

Document History			
Version	**Date**	**Contributor(s)**	**Description**
v0.1	09/10/2019	TUW, ARGOS, RU, HULAFE, QRT, CSEM	Draft
v1.0	16/10/2019	TUW, ARGOS, RU, HULAFE, QRT, CSEM	First complete version
V2.0	23/10/2019	TUW, ARGOS, QRT, CSEM	Revised version

Executive Summary

The aim of this report is to provide a method for the quantitation of the target analytes (from D2.2 – D2.4) considered valuable for the Nutrishield project. These methods were developed with a laboratory-scale experimental setup approach. They will then be integrated into the prototypes developed in D4.2 (Urine analyser prototype), D4.3 (Breath analyser prototype) and D4.4 (HM analyser prototype). Besides the methods it is also providing the spectroscopic requirements for ALPES to develop the laser sources necessary for the prototypes. The present report also targets to give an overview of the new method developed by CSEM for measuring pH in urine (potentially available also for human milk analysis).

Table of Contents

Table of Figures

List of Tables

Definitions, Acronyms and Abbreviations

Acronym	Title
ATR	Attenuated total reflection
BaF_2	Barium Fluoride
CaF_2	Calcium fluoride
CE	Counter electrode
CH_4	Methane
DW	Deionized water
EC-QCL	External Cavity Quantum Cascade Laser

ELISA	Enzyme-linked immunosorbent assay
EtOH	Ethanol
FPGA	Field Programmable Gate Array
FT-IR	Fourier-transform infrared
GC-MS	Gas chromatography–mass spectrometry
HCl	Hydrochloric Acid
HCN	Hydrogen cyanide
HMA	Human Milk Analyser
IR	Infrared
LLS	Laser light scattering
LPGC	Long path gas cell
MCT	Mercury cadmium telluride
MIR	Mid-infrared
NaOH	Sodium hydroxide
OCP	Open circuit potentiometry
OPO	Optical parametric oscillator
ppb	Parts per billion
ppm	Parts per million
PTR-MS	Proton-transfer reaction mass spectrometry
QCL	Quantum Cascade Laser
RE	Reference electrode
RMS	Root mean square
RSD	Root standard deviation
SDS	Sodium dodecyl sulphate
SDS-PAGE	Sodium dodecyl sulphate polyacrylamide gel electrophoresis
SIBO	Small Intestinal Bacterial Overgrowth
SIFT-MS	Selected ion flow tube mass spectrometry
SNR	Signal to noise ratio
SPE	Screen-printed electrode
VOC	Volatile organic compounds
WE	Working electrode
ZnSe	Zinc selenide

1. Human Milk Analyser

1.1. Definition of target analytes

Human milk is a complex biological fluid, consisting of thousands of constituents, which can broadly be categorised according to their physical or physiological properties. The composition varies among and within women and is influenced by factors such as genetic individuality, maternal nutrition, stage of gestation and lactation. Protein content is high in early secretions (15.8 g/L) and decreases to 9.0 g/L with the establishment of lactation (Picciano, 2001). Human milk proteins are divided into the whey and casein fractions, each consisting of numerous specific proteins and peptides. The most abundant proteins are casein (~3 g/L), α-lactalbumin (~3 g/L) and lactoferrin (~2 g/L) followed by secretory immunoglobulin A, lysozyme and serum albumin (Ballard and Morrow, 2013). Target analytes for the Nutrishield prototype are the proteins casein, α-lactalbumin and lactoferrin as well as the total protein content.

1.2. Reference method

The Miris HMA (human milk analyser) (https://www.mirissolutions.com/our-products) will be employed as reference method for total protein analysis. MIRIS HMA is using mid-IR transmission measurements to quantify total protein and requires a laboratory technician. It needs 3 mL of sample and takes 60 seconds. The homogenisation of the sample is ensured with an ultrasonic processor. The sample needs to be held at a certain temperature before it is transferred manually into the device with a syringe. Commercial ELISA kits for the determination of casein, lactoferrin and a α-lactalbumin will be employed for quantification of individual proteins in human milk samples.

1.3. Mid-IR Spectroscopy of proteins and peptides

Mid-IR (infrared) spectroscopy is a well-established technique for the analysis of polypeptides and proteins. The amide I band (1700-1600 cm^{-1}) originating from C=O stretching coupled to in phase bending vibration of the N-H and the amide II band (1600-1500 cm^{-1}) arising from N-H bending and C-N stretching vibrations are the most useful bands for secondary structure evaluation and quantification of proteins. Strong absorption of H_2O near 1640 cm^{-1} makes IR studies of proteins in aqueous solutions challenging. For conventional Fourier-transform infrared spectroscopy (FT-IR), very short pathlength of <10 µm are needed to avoid total IR absorption in the spectral region of water (Heinz Fabian, Maentele, & Kreutz, 1981). Particularly solutions with multiple components and complex matrices such as milks tend to clog or form air bubbles in liquid cells with such low optical path length, making robust sample handling challenging. As an alternative light source for mid-IR measurements, quantum cascade lasers (QCLs) have been introduced two decades ago (Faist et al., 1994). They provide spectral power densities several orders of magnitude higher than thermal light sources (Weida & Yee, 2011).

1.4. Laboratory-scale experimental setup

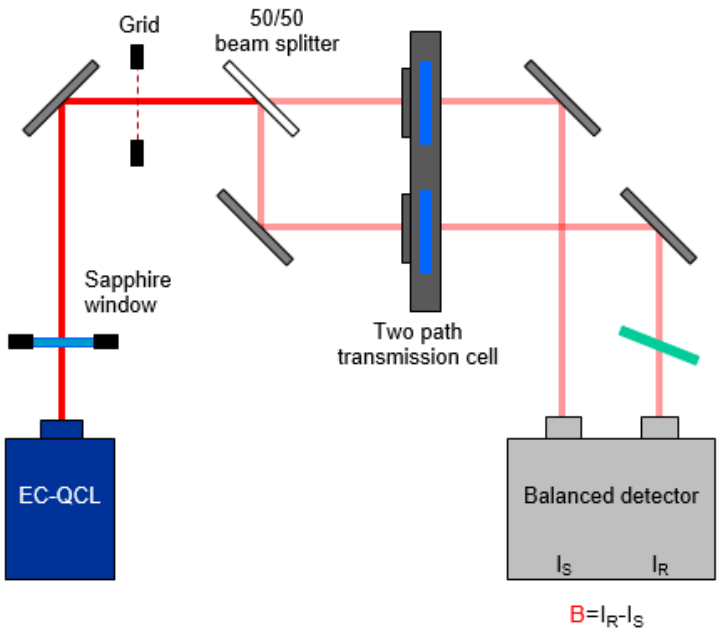

Figure 1: Laser-based IR transmission setup for analysis of the protein amide I and amide II band in milk.

It has been successfully shown, that EC-QCL lasers can be used for quantitative and qualitative analysis of proteins (Alcaráz et al., 2015; Schwaighofer, Montemurro, et al., 2018).

Within the Nutrishield project, a custom-made external cavity-quantum cascade laser (EC-QCL setup) based on (Schwaighofer, Montemurro, et al., 2018) was amended (see Figure 1*Figure 1: Laser-based IR transmission setup for analysis of the protein amide I and amide II band in milk.*) to achieve even better figures of merit. This setup consists of a water cooled external-cavity quantum cascade laser (Hedgehog, Daylight Solutions Inc., San Diego, USA). Spectra are recorded in the spectral tuning range between 1730-1470 cm^{-1}, covering the amide I and amide II region of proteins. A grid is employed to attenuate the laser intensity and a wedged sapphire window is used to selectively reduce the laser intensity in the amide II region. A pronounced innovation that could be achieved within the Nutrishield project was the implementation of balanced detection mode. For these balanced measurements, a two path-transmission cell was developed. The emitted light is divided into two beams by a beam splitter and directed into a transmission cell with two liquid compartments. The intensity of both is measured on a thermoelectrically cooled balanced MCT detector (Vigo Systems S.A., Poland). This detector provides individual outputs for the signal and reference channels as well as the balanced channel, which corresponds to the difference between the two channels. This balanced detection mode enables to reduce the noise levels introduced by the laser emission noise. The signal-to-noise ratio (SNR) is evaluated by calculation of 100% lines. Under ideal conditions, the result would be a flat line at 100% transmittance, corresponding to zero absorbance. However, several noise contributors result in a spectrum that is not a flat line but contains the noise floor of the setup. This noise can be evaluated by calculating the root-mean square (RMS) of this 100% lines. In previous EC-QCL based setups the Root Mean Square (RMS) noise of the 100% line was

~6.5*10^{-5} when employing a transmission cell with a path length of 31 µm (Schwaighofer, Montemurro, et al., 2018). With a balanced detector that uses two individual detectors which are precisely matched, unwanted noise can be further reduced by a factor of 3-4, leading to RMS noise of ~2.8*10^{-5}.

1.5. Comparison of measurement parameters between lab-scale setup and Nutrishield human milk prototype

A custom-built temperature-controlled two path transmission cell, equipped with Mid Infra-red (MIR) transparent CaF_2 windows and 26 µm path length is used for the measurements. The optical transmission path length for the Nutrishield Human Milk Analyser is dependent on the parameters of the laser source provided by ALPES and will be optimised accordingly. Table 1 summarizes the key measurement and component parameters of the laboratory EC-QCL setup and the to be developed laser source of the Human Milk Analyser.
All solutions are manually injected into the flow cell employing 1 mL disposable syringes and PTFE tubings with a diameter of 0.25 mm. For the Nutrishield Human Milk Analyser an automatic sampling system will be implemented to facilitate liquid handling.

Table 1: Key measurement and component parameters of the laboratory EC-QCL setup and the spectroscopic module of the future Nutrishield Human Milk Analyser.

	Laboratory EC-QCL setup	Nutrishield spectroscopic module for breast milk analysis
Laser emission power [mW]	20-25	up to 50
Sample interaction length [µm]	26	To be optimised
Detector detectivity [cm $HZ^{0.5}$ W^{-1}]	1.6x10^{10}	4x10^{8}
Mode of operation	pulsed	pulsed
Duty cycle [%]	50	0.5 - 50

1.6. Sample handling and preparation

1.6.1. Homogenisation

The Nutrishield Human Milk Analyser does not require any laborious sample preparation. Merely, a homogenisation step of the raw breast milk samples is required. This procedure breaks up the fat globules to decrease the average fat globule diameter and to narrow the distribution. By this, the accuracy of the results can be increased and the so-called Christiansen light-scattering effect can be minimized. The Christiansen effect is caused by large fat globules and shifts the apparent wavelength of light absorption to a longer wavelength (Di Marzo, Cree, & Barbano, 2016).

For the developed EC-QCL setup, a laboratory scale Sonicator (Branson Digital Sonified 450, equipped with a microtip horn) was used for homogenisation. An optimum of reasonably mild conditions providing a maximum homogenisation was found to be at output level 5 (~55 W) at a duty cycle of 50% with a runtime of 40 cycles (50 sec). During this process the temperature of the milk increased from initial 22°C to 44°C. Figure 2 shows Laser Light scattering (LLS) measurements performed by a Mastersizer 2000 (Malvern Instruments, Malvern, UK). Untreated raw breast milk consists a broad particle size distribution with a center at 6 µm. The size distribution significantly narrows with increasing sonication times and shifts to a center of approximately 1 µm. Figure 3 shows microscope images of untreated (A) and sonicated (B) milk. This figure confirms that there are now large fat globules present in the sonicated milk.

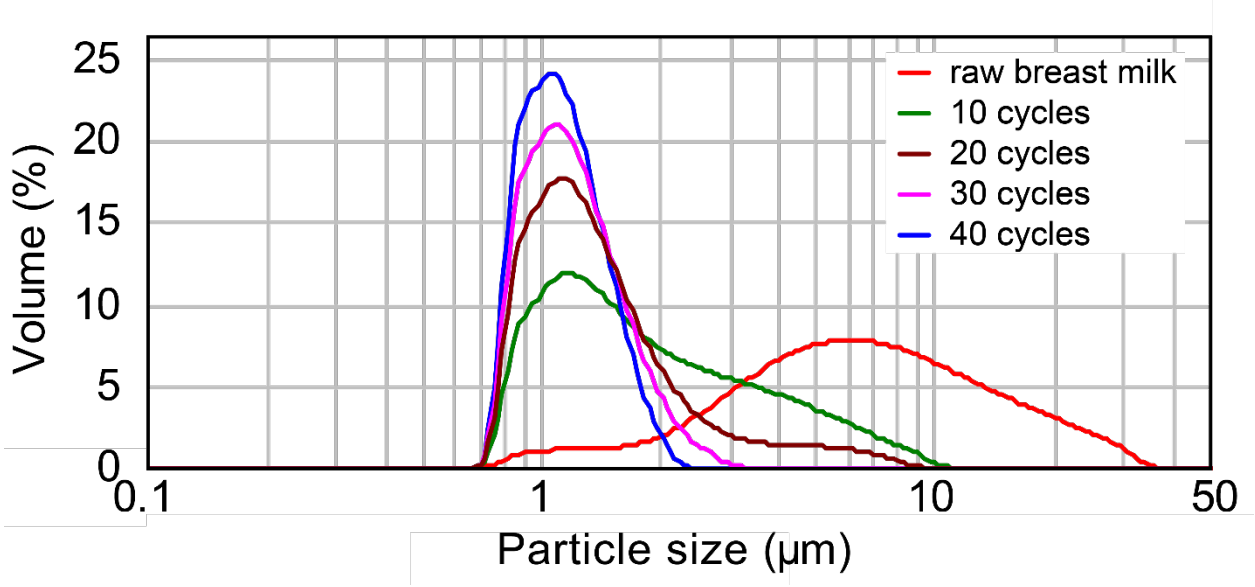

Figure 2: Particle size distribution obtained by LLS of human milk samples that were ultrasonically treated for different periods of time. The red line indicated untreated breast milk. Green, red, pink and blue lines show results of breast milk that was homogenised for 10, 20, 30 and 40 cycles.

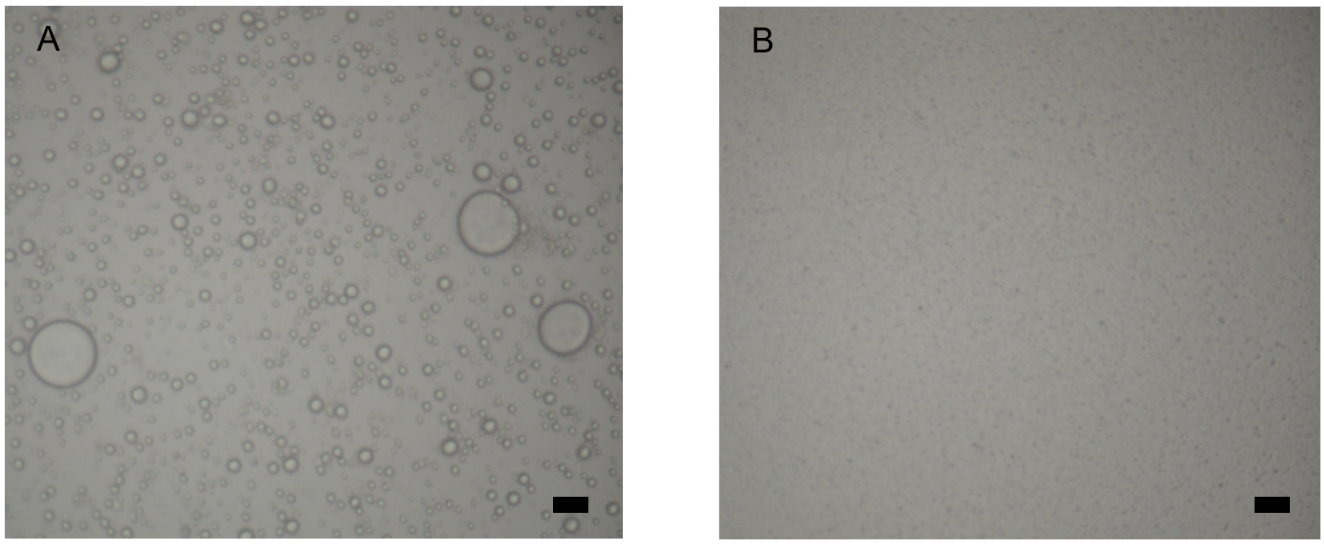

Figure 3: Microscope image of (A) untreated breast milk samples and (B) breast milk samples that were homogenised for 20 cycles. The scale bar indicates 20 µm.

1.6.2. Cleaning procedure

After each sample, the flow cell was cleaned with 1% SDS, EtOH, 0.01M NaOH and 0.01M HCl to avoid unwanted protein and fat residues in the cell.

1.7. Selection of significant wavenumbers for quantification of target analytes

The selection of individual wavelengths was performed using 15 calibration spectra with different protein concentrations of casein, α-lactalbumin and lactoferrin covering the relevant spectral range for protein analysis, which is the amide I and amide II region. (see Figure 4) These spectra were recorded employing a custom-built external cavity quantum cascade laser (EC-QCL)-based IR transmission spectroscopy setup. The concentration levels for this investigation were 1-10 mg mL^{-1} for the individual proteins and 3.25-21.50 mg mL^{-1} for the total protein content, which is the relevant concentration range for these proteins in human breast milk samples.

Partial least squares (PLS) regression was used for quantification of the individual proteins. Wavenumbers across the entire amide I and II region were used. As parameter for the wavelength selection within PLS, the selectivity ratio was employed. Parameters for evaluation the quality of the PLS analysis are the coefficients of determination for the calibrations and cross validation, which should be close to 1, such as the RMS error of calibration and leave-one out cross validation which should be rather low. *EC-QCL-IR spectra of the calibration standards used to build the PLS model and receive the best wavenumbers to be employed in the Nutrishield Human Milk Analyser.*

Table 2 shows a PLS model providing good results for the target analytes.

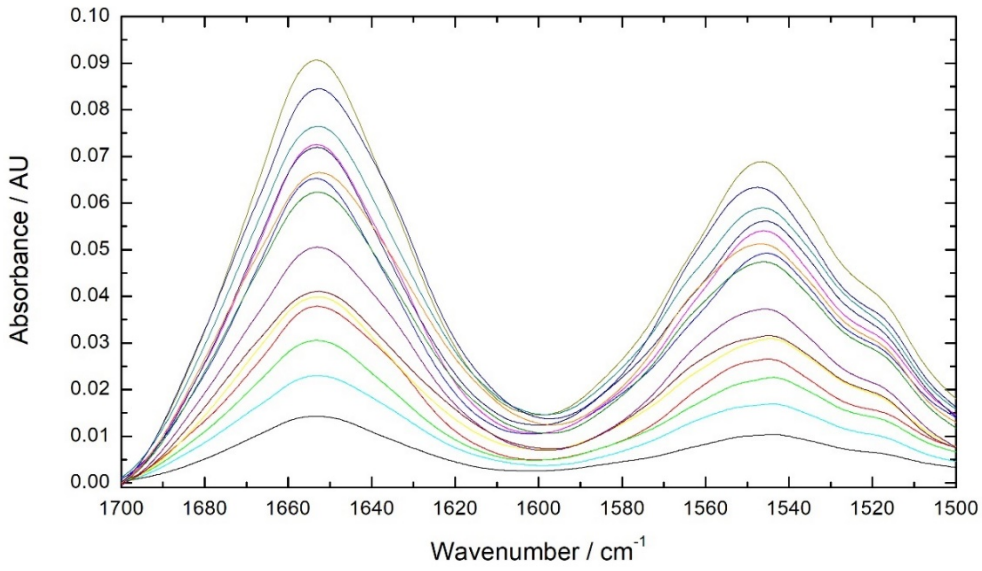

Figure 4: EC-QCL-IR spectra of the calibration standards used to build the PLS model and receive the best wavenumbers to be employed in the Nutrishield Human Milk Analyser.

Table 2: Comparison of the PLS results of the laser-based broadband IR transmission spectra and the evaluation of the selected wavenumbers.

	Casein	α-La	Lactoferrin	Total Protein
Pre-processing	MC	MC	MC	MC
Latent Var.	3	3	3	1
RMSEC [g/L]	0.47	0.19	0.27	0.26
RMSECV [g/L]	0.67	0.25	0.37	0.30
CV Bias	0.0638	-0.011	-0.02	-0.008
R^2 Cal	0.9755	0.9961	0.9912	0.9977
R^2 CV	0.9516	0.9933	0.9833	0.9968

1.8. Advantages compared to reference method and other analytical methods

Traditional methods for the analysis of proteins in human milk rely on wet-chemical sample preparation (dilution, precipitation, separation, setting pH, etc.). These methods include sodium dodecyl sulphate-polyacrylamide gel electrophoresis (SDS-PAGE) (Velonà et al., 1999), automated microfluidic SDS-PAGE (Affolter et al., 2016), high performance liquid chromatography with ultra violet detection (HPLC-UV) (Ferreira, 2007) and enzyme-linked immunosorbent assay (ELISA) (Chang et al., 2013). All of these methods are highly time consuming, intensively laborious and require trained personnel for the specific method. Moreover, they are typically location-bound to a specific lab and/or unportable instrument. The Nutrishield prototype will enable fast analysis of the individual proteins casein, α-lactalbumin, lactoferrin as well as total protein content without any wet-chemical-based sample preparation steps. The portable device will be operable with minor training and generates data within several seconds to minutes. This information can be used for guiding personalised fortification of human breast milk as well as the nutrition of lactating mothers.

2. Urine Analyser

2.1. Definition of target analytes

The constituents of urine can broadly be characterised as water, electrolytes, nitrogenous compounds, vitamins, hormones, organic acids and miscellaneous compounds. The major part is water (approximately 91-96%), followed by urea, chloride, sodium, potassium, creatinine, and phosphate (Putnam, 1971; Rose, Parker, Jefferson, & Cartmell, 2015). Target analytes for the Nutrishield Urine Analyser are phosphate and creatinine. These analytes have been selected because they are relevant for the Nutrishield project and based on their concentration range in urine, they can be detected by QCL-based sensors. The major part of phosphate is dissolved as tripotassium phosphate or as tricalcium phosphate. However, there can also

be sediments such as ammonium magnesium phosphate, which can be dissolved by acidification, making analysis of acidified urine favourable. The amount of phosphate in human urine is an indicator for various diseases. Too high concentrations can be an indicator for kidney disease, hyperathyreaoidism or too much vitamin D in the body. Too low phosphate levels may mean that the patient suffers from kidney disease, liver disease, malnutrition, alcoholism, diabetic ketoacidosis or osteomalacia (Lund Myhre, Christensen, Nicolaisen, & Nielsen, 2003; Phosphate in Urine, accessed on 24. September 2019 from https://medlineplus.gov/lab-tests/phosphate-in-urine).

2.2. Laboratory-scale experimental setup

All laboratory-scale experiments were performed using a Bruker Tensor 37 FT-IR Spectrometer (Ettlingen, Germany), equipped with a deuterated lanthanum α-alanine doped triglycine sulphate (DLaTGS) detector. The transmission experiments were performed by using a flow cell with a pathlength of 50 µm. To investigate the most appropriate window material for the Nutrishield prototype BaF_2 and CaF_2 were tested in the following experiment. For investigating their stability against sulphate, BaF_2 and CaF_2 windows (2 mm thickness) were placed into a Na_2SO_4 solution overnight. Figure 5 shows the absorption spectra of these windows. CaF_2 does not show any remarkable absorption bands after exposure to Na_2SO_4, while BaF_2 shows a broad absorption band at around 1240 cm^{-1} – 1030 cm^{-1} and a narrow band at around 1000 cm^{-1}, which are both not visible in untreated BaF_2. Since this range is of major interest for the quantification of the main components in urine, uncoated BaF_2 windows cannot be used for the Nutrishield prototype. Moreover, both window materials show absorption in the low wavenumber region. BaF_2 can be used for mid-IR spectroscopy at wavenumbers higher than 800 cm^{-1}, while CaF_2 can be used in the wavenumber range above 1000 cm^{-1}. It also has to be considered that only one CaF_2 / BaF_2 window was used in these experiments, while for the flow cell of the Nutrishield Urine Analyser, two windows are necessary meaning that the absorption effects would be even more distinctive. The result of this experiment shows, that CaF_2 is considered the better choice

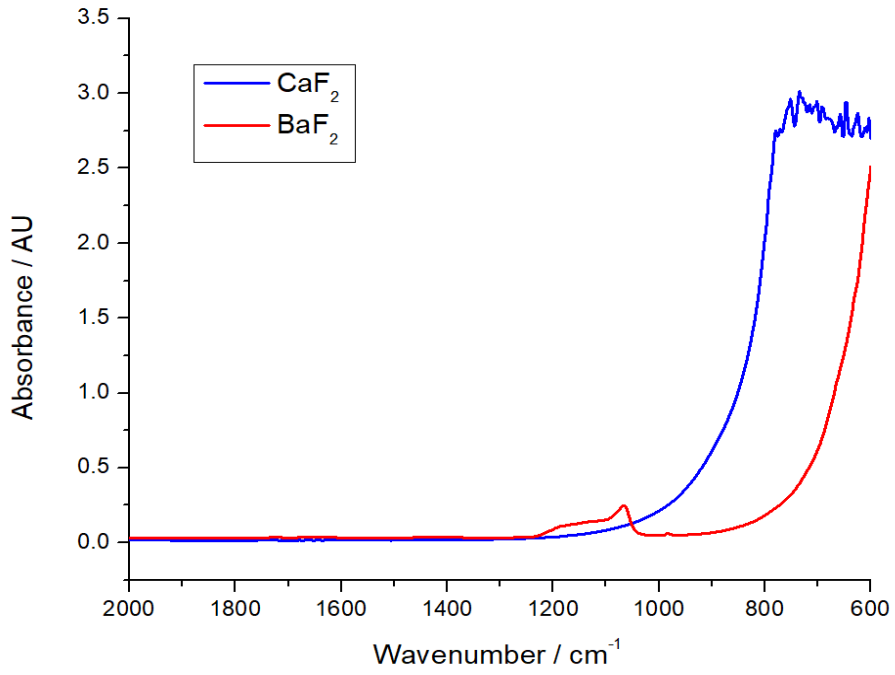

Figure 5: Absorption spectra of CaF_2 and BaF_2 after overnight exposure to Na_2SO_4.

2.3. Comparison of spectroscopy parameters between lab-scale measurements and Nutrishield Urine Analyser prototype

The optical transmission path length for the Nutrishield Urine Analyser is dependent on the laser source provided by ALPES and will be optimised accordingly. Table 3 summarizes the key measurement and component parameters of the laboratory FT-IR setup and the Urine Analyser to be developed. All solutions were manually injected into the flow cell employing 1 mL disposable syringes and PTFE tubings with a diameter of 0.25 mm. For the Nutrishield Urine Analyser an automatic sampling system will be implemented to facilitate liquid handling.

Table 3: Key measurement and component parameters of the laboratory scale setup and the spectroscopic module of the future Nutrishield Urine Analyser

	Laboratory FT-IR setup	Nutrishield setup for urine analysis
Light source emission power [mw]	~0.01	Up to 10
Sample interaction length [µm]	50	To be optimised
Detector detectivity [cm $HZ^{0.5}$ W^{-1}]	$6x10^8$	To be determined
Mode of operation	Continuous	Pulsed

2.4. Sample handling and sample preparation

Depending on the selected wavenumbers and window material, minor sample preparation needs to be performed. Either HCl in extense or a buffer solution has to be added to the sample prior to the measurements.

2.4.1. Cleaning procedure

After each sample, the flow cell should be cleaned with water, EtOH, 0.01M NaOH and 0.01M HCl to avoid unwanted residues in the cell.

2.5. Selection of significant wavenumbers for quantification of target analytes

The selection of the individual wavelengths for phosphate was performed by preparing stock solutions with concentrations of 25 mM phosphate at different pH-values (6.5, 5.5, 1.5). These solutions were measured on the FT-IR setup, equipped with a BaF_2 transmission cell.
Figure 6 shows the pH-dependency of the IR spectra for phosphate. The different spectra can be explained by the presence of various phosphate species at the selected pH-value. The IR spectra of the different ions at different pH values and their absorption maxima and vibrational modes are shown in Table 4.

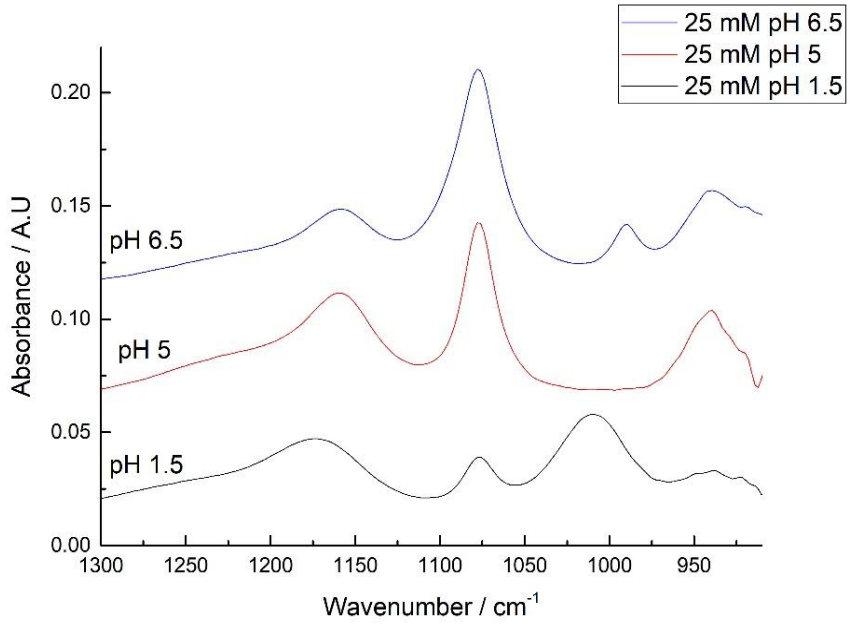

Figure 6: FT-IR spectra of phosphate at different pH values (6.5, 5 and 1.5) measured with a BaF_2 transmission cell.

Table 4: pH dependency of the phosphate species and their corresponding wavenumbers and vibrational modes (Vonach & Lendl, 1997).

pH 1.5		
Wavenumber / cm^{-1}	Species	Vibrational mode
1010	$[H_3PO_4]$	$\nu_{as}[P(OH)_3]$
1076	$[H_2PO_4]^-$	$\nu_s(PO_2)$
1173	$[H_3PO_4]$	$\nu(P=O)$
pH 5		
940	$[H_2PO_4]^-$	$\nu_{as}[P(OH)_3]$
1076	$[H_2PO_4]^-$	$\nu_s(PO_2)$
1159	$[H_2PO_4]^-$	$\nu_{as}(PO_2)$
pH 6.5		
940	$[H_2PO_4]^-$	$\nu_{as}[P(OH)_3]$
990	$[HPO_4]^{2-}$	$\nu_s(PO_3)$
1076	$[H_2PO_4]^-$	$\nu_s(PO_2)$
1159	$[H_2PO_4]^-$	$\nu_{as}(PO_2)$

Moreover, complex mixtures consisting of 1.8 g/L sulphate, 1.2 g/L phosphate, 15 g/L urea and 1 g/L creatinine were prepared to simulate the evaluation of the phosphate bands in human urine. Measurements with BaF_2 windows led to the formation of insoluble Ba_2SO_4 precipitate. Hence, the following measurements were performed with a platinum ATR (attenuated total reflection) diamond crystal.

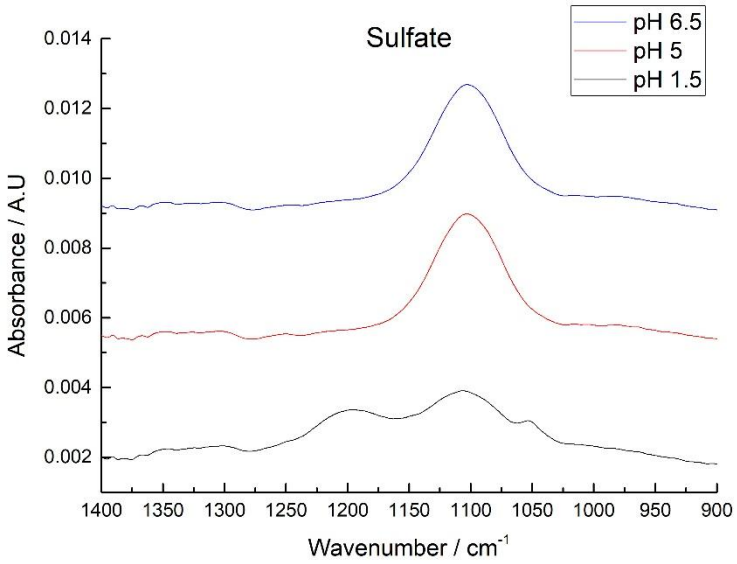

Figure 7: Spectra of sulphate at pH values of 6.5, 5 and 1.5, measured with an FT-IR spectrometer equipped with an ATR crystal.

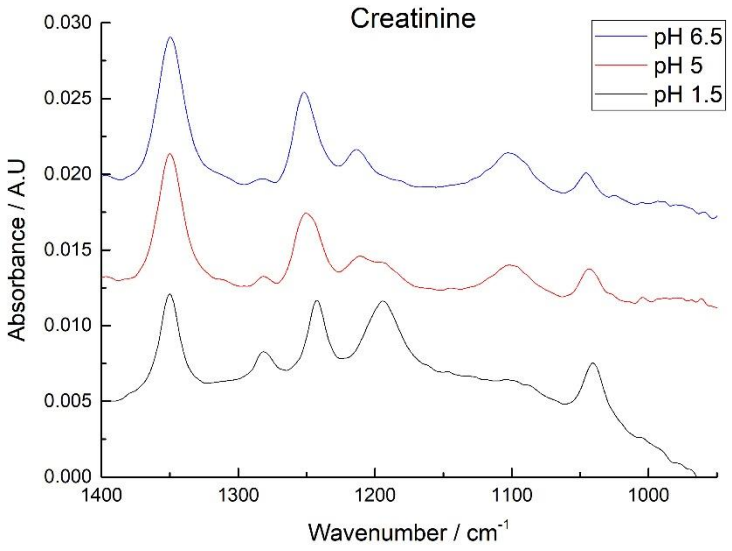

Figure 8: Spectra of creatinine at the pH values 6.5, 5 and 1.5, measured with an FT-IR spectrometer equipped with an ATR crystal.

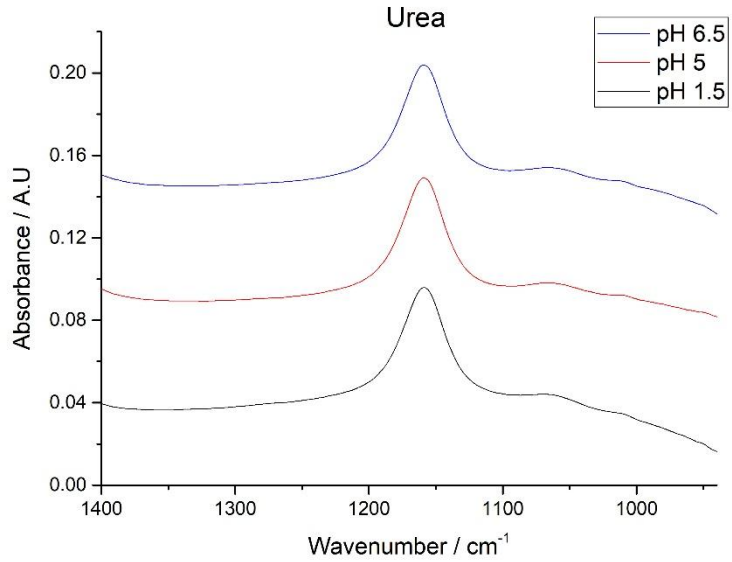

Figure 9: Spectra of urea at the pH values 6.5, 5 and 1.5, measured with an FT-IR spectrometer equipped with an ATR crystal.

Figure 7, Figure 8, Figure 9 show the FT-IR spectra of sulphate, creatinine and urea at different pH values. The quantification of creatinine can be performed at the peak with the highest intensity (1350 cm^{-1}). At this position, other major components of urine do not absorb. This peak can be measured at all tested pH-values without interfering with other components. It should however be constant among all measurements due to pH dependent intensity variations.

Overlapping IR bands from the different constituents in urine make the quantitation of phosphate challenging. An evaluation of the phosphate band with the highest intensity at around 1076 cm^{-1} is not

possible, due to absorption of sulphate at this position. The peaks at wavenumbers 1173 cm^{-1} and 1159 cm^{-1} overlap with the urea band, meaning that they also cannot be used for the Nutrishield Urine Analyser. An evaluation at 1010 cm^{-1}, pH 1.5 or an evaluation at 940 cm^{-1}, pH 5 would be possible.
Figure 10 shows linear calibration functions of phosphate solutions with different concentration levels for bands at 940 cm^{-1} (pH 5) and at 1010 cm^{-1} (pH 1.5). Both bands show good correlation and signal intensity. The main advantages of measuring at 1010 cm^{-1} would be that CaF_2 can be used as window material which is stable against urine. On the other hand, HCl in high amounts has to be added to the samples before analysis. Measuring at 940 cm^{-1} by using CaF_2 windows is not possible due to CaF_2 absorbance at this position. PE coated BaF_2 windows would be one opportunity to overcome this problem. It has however turned out to be more challenging than expected to find a supplier for such coated windows. Moreover, an exact control of the pH-value would be necessary. Other possible window materials would be ZnSe or diamond which do not absorb in the region of interest. The high cost of diamond windows is however a considerable drawback. Furthermore, the high refractive indices of ZnSe and diamond could lead to interferences with the laser source and higher noise. Here, wedged windows would be necessary.

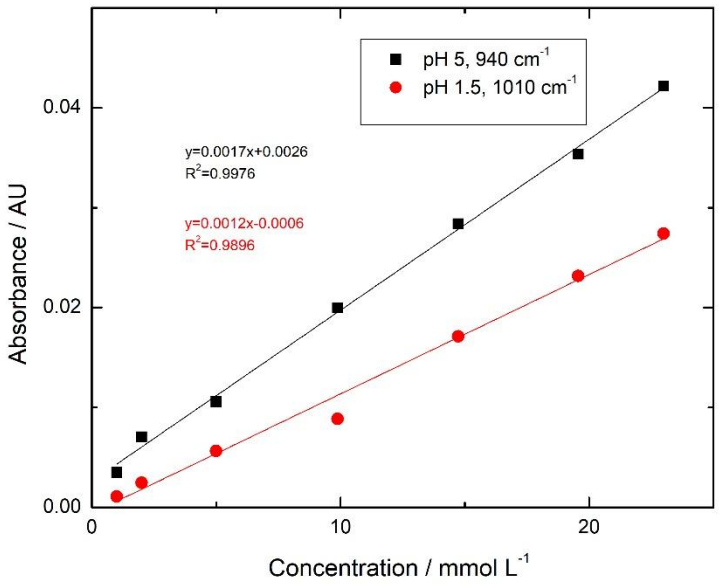

Figure 10: Linear calibration functions for different phosphate concentrations at the peak maxima of 940 cm^{-1} (pH 5) and 1010 cm^{-1} (pH 1.5).

Figure 11 shows the absorption spectra of sulphate (1.8 g/L), phosphate (1.2 g/L), urea (15 g/L), creatinine (1 g/L) and a mixture of these components with same concentrations. All solutions were measured at a pH value of 1 with a FT-IR spectrometer, equipped with a CaF_2 transmission cell. The red lines indicate the selected wavenumber of 1350 cm^{-1} for creatinine and 1010 cm^{-1} for phosphate. At these wavenumbers, other major components of urine do not absorb.

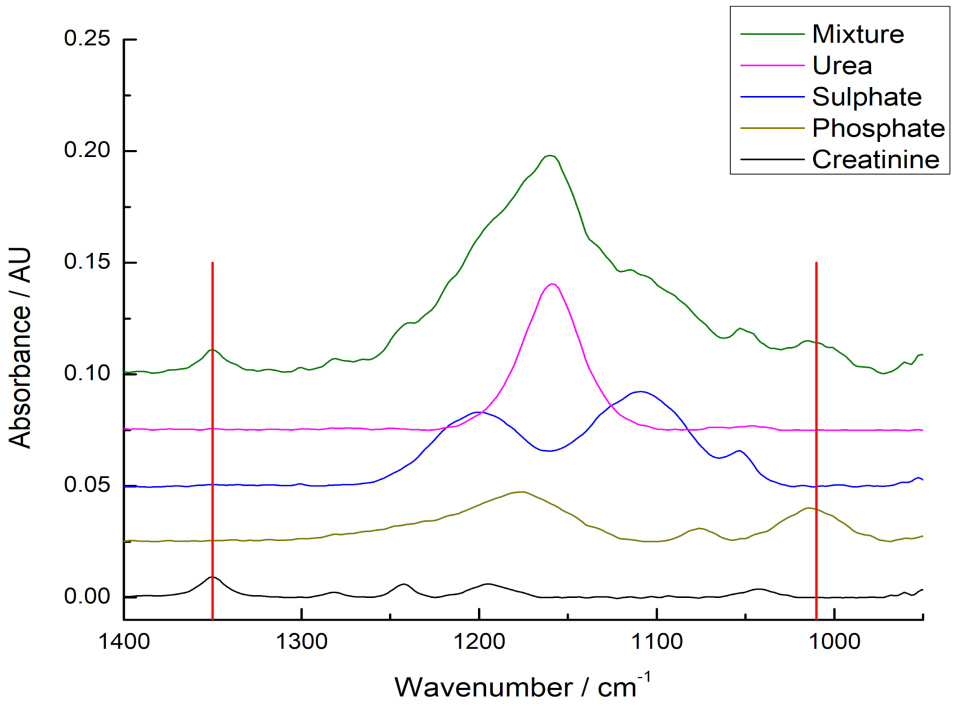

Figure 11: Spectra of urea, sulphate, phosphate, creatinine and a mixture of these compounds at pH 1 measured with an FT-IR spectrometer equipped with CaF_2 transmission cell.

2.6. Reference method

Colorimetric determination after reaction of inorganic phosphorus with ammonium molybdate will be employed as reference method for phosphate analysis. The Jaffe Method (reaction with picric acid) will be employed for the quantification of creatinine.

3. Custom made disposable pH sensor for urine monitoring

In Chapter 2 the analysis of urine using mid-IR spectroscopy was described. The method in Chapter 2 will be integrated into a prototype developed by QRT. The EC-sensor, developed by CSEM, is used as an additional tool for HULAFE in later studies to measure the pH of urine. It will not be part of the integration of QRT.

Since the urine sample volume to be collected and processed within the targeted studies scheduled in the current project is going to be 100 μl the state-of-the-art instrumentation (i.e. pH meter) appears to be not ideal since it requires a higher amount of sample (i.e. minimum 2-5 ml) available to be processed in order to correctly estimate its pH value. CSEM is going to provide a custom-made disposable pH sensor, tailored for the present requirements in urine. The CSEM-made sensors require only few microliters (i.e. 50-100 μl) of the total amount (still to be defined) of sample. The response time of the sensor is between 3-5 minutes for each sample with additional 10-15 minutes for the pre-calibration step.

3.1. Laboratory-scale experimental setup

All laboratory-scale experiments were performed as follows:

3.1.1. Screen printing electrodes

- The sensor is a screen-printed electrode (SPE) made up of 3 electrodes (see Figure 12):

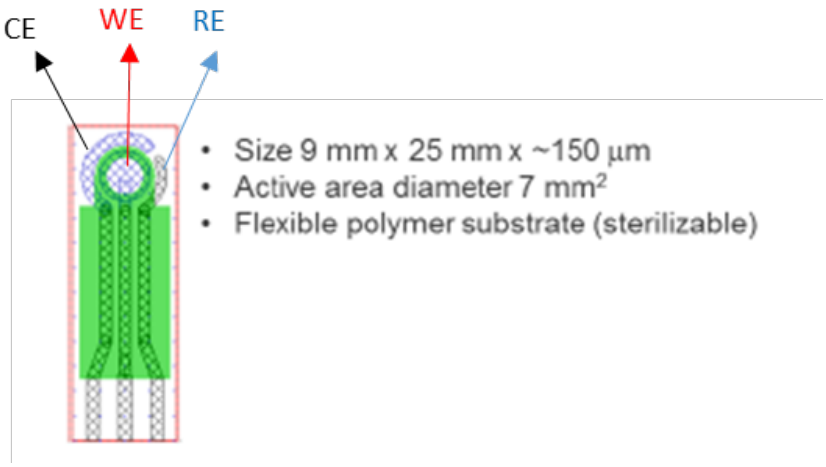

Figure 12: Schematic representation of the SPE used in this study.

i. Graphite working electrode (WE)
ii. Graphite counter electrode (CE) – not used for the pH measurements
iii. Silver/Silver-Chloride pseudo-reference electrode (RE)

- The sensor is printed on 125 µm thick PET flexible substrate. The pH-sensitive part is located on the WE.
- The sensors were printed using the screen-printing instruments (DEK248, DEK Align 4, FIAC air compressor; BINDER Incubator).
- The WE of the sensor has been functionalised with the pH sensitive layer.
- The sensors once prepared and functionally verified, were stored under vacuum at room temperature away from any light exposure.

3.1.2. Electrochemical equipment

- PalmSens Emstat3 device (from PalmSens Compact Electrochemical Interfaces) has been used for the measurements (see Figure 13).
- Open Circuit Potentiometry (OCP) has been used as technique.

Figure 13: Emastat3 instrument used for the measurements (picture taken from PalmSens Compact Electrochemical Interfaces Company website: https://www.palmsens.com/product/emstat-blue/).

3.2. Sample handling and preparation

In this preliminary study, one urine sample has been tested with three different disposable pH sensors. The urine sample has been tested with and without filtration previous to the measurement and the sensor's response has been compared. No significant difference (i.e. 0.05 pH units) was observed in the pH estimation of the filtrated and not filtrated urine sample. This means that the urine samples do not necessary require a pre-treatment prior to analysis. Of course, a higher number of urine samples needs to be tested in order to clearly confirm the mentioned statement.

3.2.1. Protocol of the measurements

The following protocol has been applied for the measurements:

- The sensor was inserted into the instrument as shown in Figure 13.
- The sensor prior to urine tests needs to be calibrated with standard solutions (i.e. pH 8, 6, 4) prepared using citrate phosphate buffer.
- Each calibration solution is monitored for about 3-5 minutes using the sensor. The total time for a three-point calibration is around 10-15 minutes.
- After calibration the sensor is ready for use.
- Each urine sample is monitored about 3-5 minutes.

- At the end of each urine sample (i.e. filtrated and not filtrated) measurement a new calibration curve was performed in order to check the sensor's performance.

The readout of the sensor can be displayed on the screen of a laptop, tablet or smartphone. In the present study a laptop has been used for displaying the results of analysis (i.e. calibration curves and urine processing). In Figure 14 a general view of the data acquisition with the CSEM pH sensors is reported.

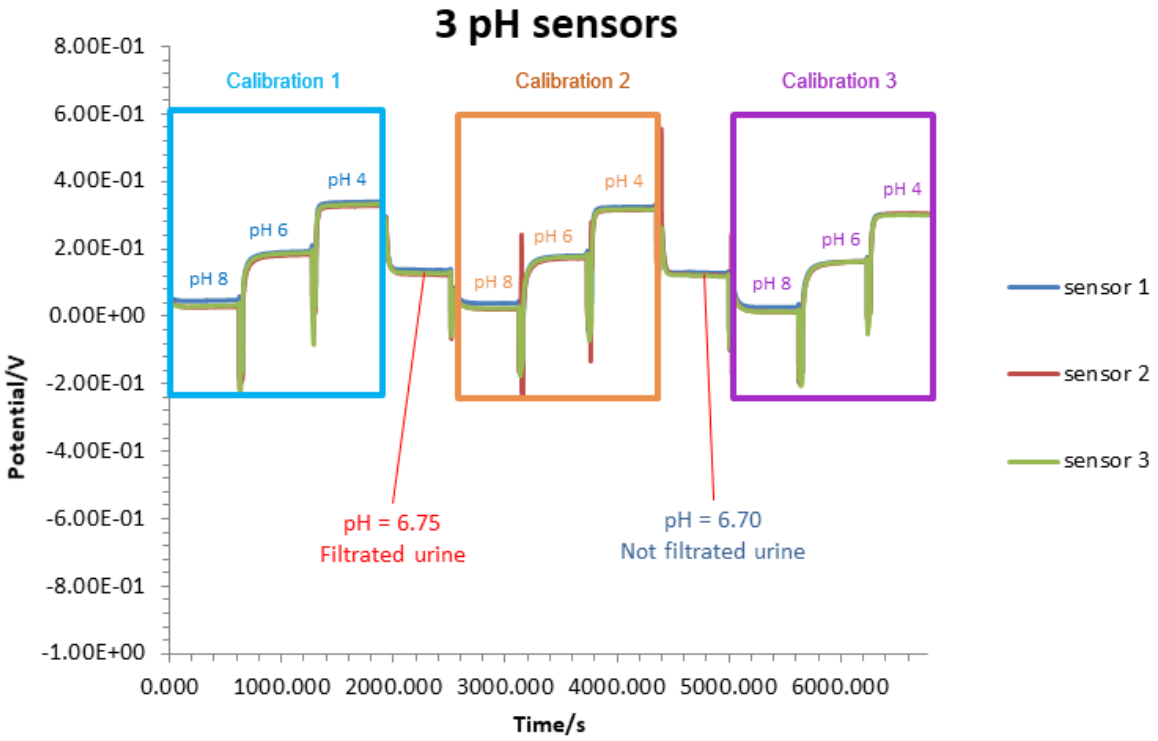

Figure 14: Potentiometric (i.e. registering the potential in V versus time) measurements performed with the Emstat3 device. The test was made in triplicate (i.e. three pH sensors). All sensors were tested as follows: a) Cyan: Pre-calibration of the sensor, b) Orange: Calibration of the sensor after testing the filtrated urine sample, c) Purple: Calibration of the sensor after testing the same urine sample not filtrated.

3.2.2. Cleaning procedure

Washing steps with deionized water (DW) in between the different urine samples (i.e. filtrated and not filtrated) monitoring has been taken place.
After the first urine analysis (i.e. filtrated urine sample) the sensors were calibrated again prior to the next urine test (i.e. not filtrated urine sample). In figure 17 the average value (i.e. three sensors included) of the calibration curves (i.e. before, during and after urine monitoring) is reported.

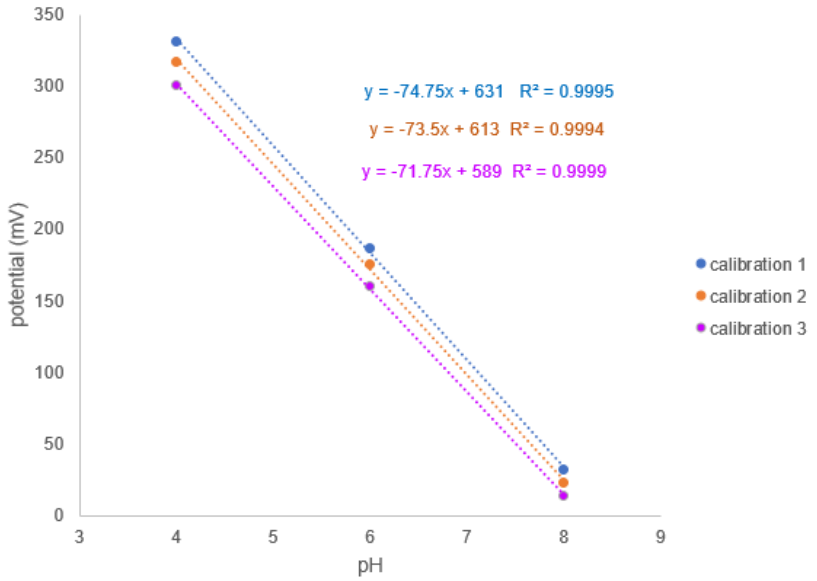

Figure 15: The mean (i.e. three sensors) value of potential registered after testing each pH solution used as calibrant (i.e. pH 8, pH 6 and pH 4) was used for the calibration curves. a) Cyan: Pre-calibration of the sensors, b) Orange: Calibration of the sensor after testing the filtrated urine sample, c) Purple: Calibration of the sensor after testing the same urine sample not filtrated.

4. Breath analyser

4.1. Target analytes

Exhaled breath consists of hundreds of gaseous compounds, including inorganic compounds (e.g., ammonia, nitric oxide, hydrogen sulfide) and volatile organic compounds (VOCs), arising from their normal body metabolism. Endogenous emissions reflect the changes in the internal metabolism when illness occur, but can also vary in response to various (external) stimuli. Although many exhaled compounds potentially reflect the physiological and pathophysiological conditions related to various diseases, only some VOCs have been established as biomarkers. Within this project we shall focus on detection of HCN and CH_4. Both gases are related to the colonic fermentation and the activity/presence of bacteria and other microorganisms in the guts. Diet, as well as low/ high nutritional status have a strong influence on the activity of these microorganisms and subsequently, on the concentrations of the metabolites produced.

4.1.1. Hydrogen Cyanide

The concentration of hydrogen cyanide in human breath typically ranges from several parts per billion (ppb) to tens of ppb. Systemic breath HCN may originate from metabolism, microorganisms, neutrophil-mediated cyanide generation and enzymatic activity, or from exogenous sources such as food containing

cyanogenic glycosides and exposure to tobacco smoke or combustion gases. Hydrogen cyanide is also an important biomarker for bacterial infections (Schmidt 2011, Neerincx 2015) and bacterial activity in the guts.

4.1.2. Methane

Methane is contained in environmental air at a level of 1.8 - 2 ppm. It is also an endogenous compound, being a by-product of carbohydrate fermentation by intestinal microorganisms (e.g. archaea). Many studies have reported correlations between breath methane levels above the ambient methane and diseases such as irritable bowel syndrome, large bowel cancer, and constipation. It indicates indigestion in infants, intestinal upset and/or colonic fermentation. A combined hydrogen and methane breath test has been shown to be superior for the diagnosis of carbohydrate malabsorption syndromes and SIBO. These tests are simple and safe alternatives compared to more invasive procedures such as biopsies and/or obtaining aspirates for culturing (De Lacy Costello 2013).

4.2. Selection of wavenumbers for the target analytes

The method of measuring the target analytes is Mid-IR spectroscopy. The absorption lines of Methane (CH_4) and hydrogen cyanide (HCN) are highest in the 3000 to 3300 cm^{-1} spectral range. The absorbance bands were selected based on the following criteria:

- Strong absorption
- Bands which can be resolved at ambient pressure and temperature
- No or little interference with other VOCs, CO_2 and H_2O

As a result, the following wavenumbers were selected:

- HCN: k = 3331.6 cm^{-1} (alternative band: 3287.3 cm^{-1})
- CH_4: k = 3086.0 cm^{-1}

The specifications for the laser remain as follows:

- tunable by about 1 cm^{-1} around the peak wavelength (for HCN and CH_4)
- the laser radiation must be single mode
- polarised
- low susceptibility to back reflection
- collimated
- the laser power should be > 5 mW within the tuning range
- the laser emission should be continuous

As H_2 is not IR- active, a different detection method needs to be chosen, e.g. on an electrochemical basis.

4.3. Schematic function diagram

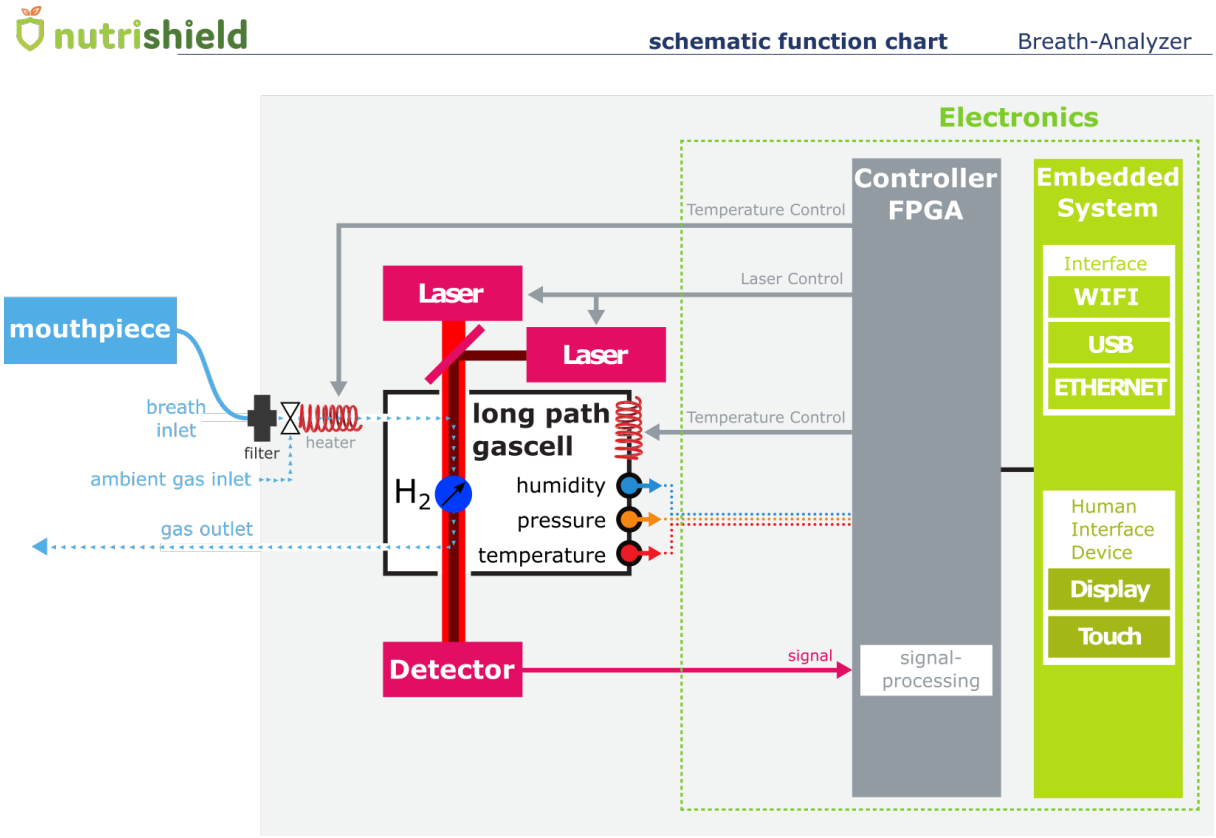

Figure 16: schematic function chart of breath analyser

As can be seen in the schematic picture (Figure 16) the breath analyser consists of a number of assemblies:

- Mouth piece with flexible hose and protective filter and heater
- Thermostated long path gas cell with
  - dual laser assembly and detectors,
  - Hydrogen sensor
  - Electronic control (Field Programmable Gate Array (FPGA))
- Human interface and external interfaces

In contrary to the analysis of body fluids breath can be analysed online. The person, whose breath is to be analysed, breathes via an exchangeable mouthpiece into the device. A filter downstream protects the sensitive optical components of the analyser from particles and moisture. Breath will be kept at elevated temperature by a heater and passed to the temperature-controlled gas cell. The temperature of the cell will be close to body temperature in order to prevent condensation of moisture and ensure repeatable measurement conditions. A valve and a small pump allow passing ambient air through the gas cell, for monitoring baseline conditions.
In order to analyse the gases of interest in exhaled breath laser radiation with specific wavelength passes through the gas cell.

The concentration of methane and hydrogen cyanide of the breath contained in the gas cell will be analysed by molecular spectroscopy at two distinct wavenumber positions requiring two well defined laser lines. The concentration of hydrogen will be recorded by a to be determined sensor. The wavelength of the laser radiation is determined by the laser's temperature and current, which are controlled by the electronic circuit. A controlled change of temperature and current facilitate the tuning of the wavelength across the selected absorbance bands of methane and hydrogen cyanide. The radiation emitted by the two lasers is coupled into the long path gas cell (LPGC), it interacts with the gas to be analysed and the reduced intensity of the radiation is detected by the photodiodes. Simultaneously to the tuning of the lasers the detector signal is acquired. The use of a long path gas cell ensures a long interaction path of the laser radiation with the gas molecules facilitating the required sensitivity. Temperature, pressure and humidity of the gas cell will be monitored to allow a very precise measurement of the gas concentrations of methane and hydrogen cyanide. A commercial sensor will be used to measure the concentration of hydrogen in breath.
The custom designed FPGA will control the measurement, while the microcontroller will handle the user interface and at a later stage data transfer (within the project data will be transferred manually).

4.4. Measurement protocol

4.4.1. On-line analysis

The on-line analysis will allow acquiring real time monitoring of the dynamic change of concentration of the analytes under observation. The concentration of the biomarkers recorded may depend on the concentration of VOCs in the environment. Therefore, it is essential to determine also the concentration of the analytes in the vicinity of the person. Knowing the concentration of the analytes in the inhaled air of the person allows a correction of the concentration of the analytes in the exhaled breath. Therefore, the measurement protocol will include the analysis of the ambient concentration of methane, hydrogen and hydrogen cyanide by using the gas inlet of the ambient air prior to the analysis of the exhaled breath. After this baseline measurement the breath sample of the person is allowed to enter the gas cell. Depending on the mode of operation the breath is analysed continuously while breathing or the alveolar volume of the breath is selected and analysed. The concentration values are displayed on the screen and stored along with date/time and the id of the person.

4.4.2. Off-line analysis

For the off-line analysis, the procedure will be as follows:
The monitoring of the gases of interest in the environmental air is performed as described in the on-line analysis. A Tedlar® bag with a stored breath sample is connected via a short adapter with the breath analyser. The breath sample contained in the bag is slowly transferred into the gas cell by exerting a slight pressure to the bag. Then the analysis as described in the on-line analysis will be performed.

4.4.3. Sampling with Tedlar® bags

Exhaled breath contains hundreds of volatile organic compounds (VOCs) which can reveal important information about the current health status of an individual. One of the main advantages of breath testing

is that it is non-invasive, which makes it a very attractive sampling method especially when working with children.

Here we present a protocol for the collection and analysis of exhaled breath VOCs in children aged 8 – 15. We measured the breath samples using three instruments: Proton Transfer Reaction Mass Spectrometry (PTR-MS), laser-based photoacoustics methane and ethylene detectors, respectively. Here the sampling protocol developed is described and its reproducibility demonstrated.

All children followed the same sampling procedure for the collection of breath samples. Each participant was asked to not eat for at least one hour prior to sampling, then rinsed their mouth with water prior to sampling. Each breath sample consisted of two mouth exhalations through a bacterial mouthpiece (GVS UK) connected to a commercial breath sampler (Loccioni®) into a 3 L Tedlar® bag (EU sample bags). The breath sampler meets the American Thoracic Guidelines (ATS) for collecting breath by providing a back pressure of 10 cm H_2O, to ensure soft palate closure and prevent nasal contamination, and allowing the subject to maintain constant exhalation flow (Thornadtsson et.al. 2015).

Briefly, the breath collection line consists of a bacterial filter, a CO_2 sensor and a calibrated buffer pipe and monitored continuously the mouth pressure and CO_2 concentration during an exhalation. The CO_2 concentration and airway pressure profiles are displayed in a graphical form on the screen of the sampler (Mandon et. al., 2012). The first 150 ml of breath (dead space portion) is collected into a smaller discard bag; the rest of the breath (end tidal portion) is then collected into the 3 L Tedlar® bag placed at the end of the pipe.

After a few tests on the exhalation procedure, the participants were asked to exhale while having visual feedback by a coloured dynamic bar on the sampler screen (LED lighting system) indicating suitable pressure for the sampling (i.e. red is too fast, green is the optimal exhalation flow) (Figure 17). During the sampling procedure it is important that the mouth pressure is kept constant, enabling the participant to maintain a constant expiratory flow. Two room air samples were collected, one prior to the sampling and one straight after sampling. The bags were transported to the laboratory for analysis. The samples were analysed within 2 hours of collection to minimize losses from the bags, studies show the bags can be stable for up to 6 hours (Steeghs, 2007).

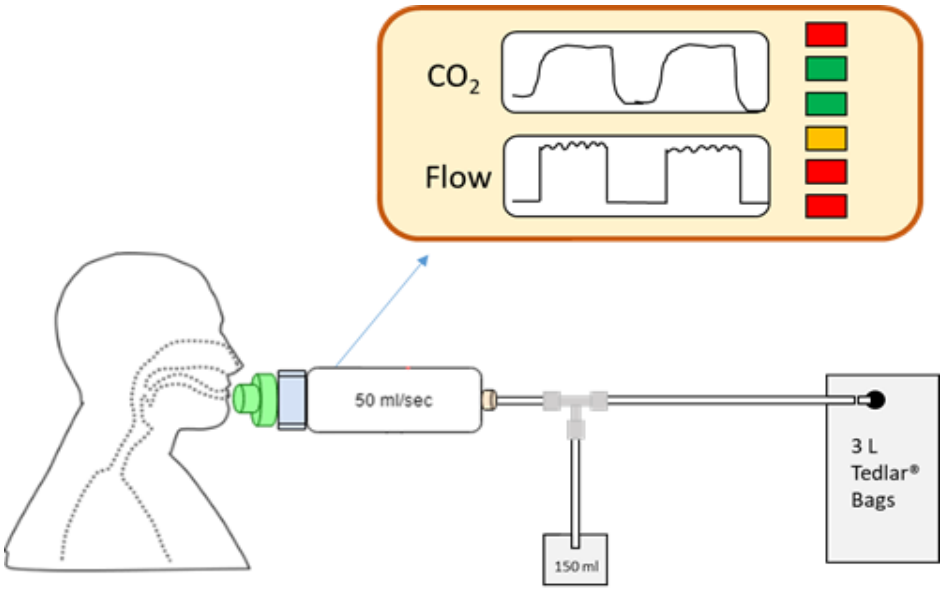

Figure 17: Off-line sampling in tedlar bags

Table 5: Average relative standard deviation (%) of 2 breath samples per participant

Compound	Average RSD % between duplicate breath samples
Acetone	3.6
Isoprene	4.9
Methanol	4.2
Ethanol	10.7
Acetaldehyde	4.7
Dimethyl Sulphide	5.3
Ethylene	10.6
Methane	2.2
Water content	1.36

In Table 5 compounds showed less than 5 % RSD between duplicate samples, with only ethanol and ethylene showing higher variation (>10%). The concentrations of ethylene are very low, typically less than 2 ppb, therefore a small absolute difference in the signals between the bags may be over represented as a relative standard deviation between samples. Ethanol has been shown to decrease significantly over time in breath samples stored in Tedlar® bags when compared with other VOCs that are stable for longer, this may explain the 10% relative standard deviation between samples.

4.5. Reference Methods and Advantages of the Nutrishield analyser

4.5.1. State of the Art

Breath analysis is not yet a well-established analytical method for diagnosis. It is currently only applied for specific indications e.g. for the evaluation of the metabolic capacity of the liver, for the determination of the presence of *Helicobacter pylory* etc. In these cases, the isotopic ration of $^{13}C/^{12}C$ of carbon dioxide in exhaled breath is being analysed. To our knowledge, methane in exhaled breath is analysed by one commercial instrument only, a commercial instrument for the analysis of HCN in exhaled breath is not available.

Breath analysis for research purposes is usually performed using sophisticated laboratory instruments. Several methods are currently employed for exhaled volatiles detection, among which mass spectrometry (e.g. gas chromatography mass spectrometry, GC-MS) is the most widely used analytical tool. However, the GC-MS-based instruments are limited to laboratory settings, do not allow online sampling and have a relatively long analysis time (in the order of tens of minutes). For these reasons, extensive research has been conducted to develop other methods that can be used to perform rapid, sensitive, online analysis in a clinical setting, preferably for many volatile compounds simultaneously. Proton-transfer reaction mass spectrometry (PTR-MS) (Del Rio, 2015), selected ion flow tube mass spectrometry (SIFT-MS) (Dryahina, 2018), gas chromatography combined with ion mobility spectrometry (GC-IMS) (Mochalski, 2018) and secondary electro-spray ionization mass spectrometry (SESI-MS) (Gaugg, 2016) are few examples of online mass-spectrometric (MS) methods currently used for breath analysis. In spite of these advances, there is a continuous need for miniaturized devices, in addition to the consideration of an affordable, accurate and user-friendly instrument that should provide fast response, preferably in real-time.

4.5.2. Calibration of the breath analyser

The current reference instruments are the laboratory instruments. Sophisticated research instruments based on e.g. mass spectrometry or laser spectrometers using molecular absorption offering high sensitivity and accuracy are available at a number of research institutions. Therefore, we plan to prove the accuracy and sensitivity of the Nutrishield analyser in two steps. Step one uses calibrated gas mixtures and step two will compare results from the Nutrishield breath analyser with results from identical samples evaluated at a research laboratory.

RU and TUW plan to validate the performance of the breath analyser using alternative (analytical) methods, e.g. calibration test samples as well as stored breath samples will be run in parallel with the Nutrishield breath analyser and the established lab equipment.

4.5.3. Advantages of the Nutrishield Breath Analyser

From clinical standpoint, there is a demonstrated need for breath analysis particularly real-time portable devices (point-of-care testing, personalised medicine). From an instrument standpoint, progress has been made too. Devices suitable for routine clinical use are at various stages of development (Henderson, 2018). Breath analysis is not yet a routine analysis, thus the concentration of e.g. CH_4 and HCN in breath are not routinely analysed.

The laser-based sensors proposed within this project will allow on-line measurements and, especially for CH_4, no pre-concentration steps are foreseen. Depending on the laser properties and the detection scheme, also HCN could be sensitively measured at 3287 cm^{-1}.
Currently, laboratory set-ups using OPO-based photoacoustic spectroscopy (at 3.3 - 4 µm) or diode laser-based cavity ring down spectroscopy (at 6504.3–6504.5 cm^{-1}) are employed for detection of HCN. No compact and/or commercial instruments are presently available.
For CH_4 detection, several electrochemical sensors are commercially available and one company has an analyser for both CH_4 and H_2 measurement on the market for breath analysis (Bedfont Ltd.). The applications might be limited due to the measuring procedure (the patient is asked to inhale deeply and exhale into the device, the measured breath being thus mixed) and the required stability for the ambient conditions (constant temperature and air currents). Another limitation is given by the limited sensitivity of the device. Furthermore, no information on gas concentration dynamics could be monitored (but discrete measurements).
The Nutrishield Breath Analyser combines the analysis of 3 biomarkers in one portable instrument. The Analyser is lightweight and compact. The analysis can be performed in a short time, on-line, usually in less than one minute. Dynamic measurements will be possible, presumably allowing to monitor the change of concentration while breathing.
The analyser can easily be operated, no lab personnel will be needed. Consumables are limited to a mouth piece and occasionally an (air) filter.

5. Conclusions

It was shown in this deliverable that the methods developed with the laboratory-scale experimental setups can be used for the integration of spectroscopy unit and sample preparation in the prototypes being part of D4.2, D4.3 and D4.4.

5.1. Human Milk analysis

The target analytes of human milk are total protein and the three most abundant proteins casein, lactoferrin and α-lactalbumin. The experimental setup used a commercially available EC-QCL (Daylight Solution) and a path length of 26 µm. A balanced detection setup was applied to achieve a better S/N ratio and therefore a better accuracy and in the end a better limit of detection.
To quantify the target analytes a PLS model was set up and 10 wavenumbers were chosen with 13 calibration samples.
Raw human milk needs sample preparation, since the fat globules in the milk can lead to light scattering and a shift of the peak position to longer wavelengths. This was achieved by using a commercially available sonicator.

5.2. Urine analysis

Using mid-IR spectroscopy, the analytes measured will be phosphate and creatinine. Measurements with a flowcell of 50 µm thickness and BaF_2 windows with a FTIR were conducted. Phosphate and creatinine in a buffer solution at different pH levels were measured, as well as different other urine components, like urea and sulphate. The optimum wavenumber for creatinine was 1350 cm^{-1} and for phosphate, whose peak position is dependent on the pH of the urine, either 940 cm^{-1} (pH = 5) or 1010 cm^{-1} (pH = 1). During these experiments, a white film on the BaF_2 windows was observed. After further investigation, the white film was identified as $BaSO_4$. This observation was important for the Nutrishield analyser in choosing the suitable components. The options are:

- Using coated BaF_2 and measuring at 940 cm^{-1} at a pH of 5 (setting the pH at high accuracy is necessary)
- Using CaF_2 and measuring at 1010 cm^{-1} at a pH of 1 (no pH measurement necessary, since adding an excessive amount of HCl is ensuring the pH)

5.3. Electrochemical sensor by CSEM

State-of-the-art pH measurements with a pH meter needs a minimum of 2-5 mL sample. The amount of urine for the measurements is limited to 150 – 200 µl and therefore no conventional pH meter can be used in this case. CSEM is producing electrochemical sensors, which is a screen-printed electrode made up of 3 electrodes. To be able to measure the pH with the EC-sensor, as electrochemical Interface is necessary, as well as an open circuit potentiometry.

In this preliminary study, tailored disposable CSEM pH sensors have been prepared and tested for urine monitoring. The goal was to understand the sensor behaviour in terms of operational stability and establish the need of a sample pre-treatment or not after processing real urine samples.
The results obtained in this study demonstrated that the CSEM pH sensors are stable for approximately 1 hour of continuous measurements (i.e. calibration curves and urine monitoring) and they do not necessary require a pre-treatment (i.e. filtration). All the above-mentioned requirements totally cover the targeted disposable use of the pH sensors within the “Nutrishield” project.
The pH sensor by CSEM will be used as an additional tool for the Nutrishield platform, but will not be part of the integration into the urine analyser developed by QRT.

5.4. Breath Analyser

Using mid-IR spectroscopy, the concentration of hydrogen cyanide and methane will be determined. The usable absorption lines were determined by modelling the infrared transmission properties of breath allowing the specification of the lasers to be provided by ALPES. The concentration of hydrogen will be determined online using a commercial sensor. The measurement procedure for online and offline analysis of methane and hydrogen cyanide in exhaled breath is described.

6. References

A. Thornadtsson, A.H. Neerincx, M. Högman, C. Hugen, C. Sintnicolaas, F.J.M. Harren, P.J.F.M. Merkus, S.M. Cristescu, Extended nitric oxide analysis may improve personalized anti-inflammatory treatment in asthmatic children with intermediate FENO50, J. Breath Res. 9(4):047114 (2015)

Affolter, M., Garcia-Rodenas, C. L., Vinyes-Pares, G., Jenni, R., Roggero, I., Avanti-Nigro, O., … Favre, L. (2016). Temporal changes of protein composition in breast milk of Chinese urban mothers and impact of caesarean section delivery. *Nutrients*, *8*(8).

Alcaráz, M. R., Schwaighofer, A., Kristament, C., Ramer, G., Brandstetter, M., Goicoechea, H., & Lendl, B. (2015). External-Cavity Quantum Cascade Laser Spectroscopy for Mid-IR Transmission Measurements of Proteins in Aqueous Solution. *Analytical Chemistry*, *87*(13), 6980–6987.

Ballard O and Morrow AL. (2013) Human Milk Composition: Nutrients and Bioactive Factors. *PediatricClinics of North America*. 60: 49-74.

Ballard, O. & Morrow, A. Manuscript, A., & Factors, B. (2014). *NIH Public Access. Human Milk* ComposiyionComposition: Nutrients and Bioactive Factors*. Pediatr Clin North Am. 60*(1), 1–24.

Chang, J. C., Chen, C. H., Fang, L. J., Tsai, C. R., Chang, Y. C., & Wang, T. M. (2013). Influence of prolonged storage process, pasteurization, and heat treatment on biologically-active human milk proteins. *Pediatrics and Neonatology*, *54*(6), 360–366.

De Lacy Costello B. P., Ledochowski M. and Ratcliffe N. M. 2013

Del Rio R.F., M. E. O'Hara, A. Holt, P. Pemberton, T. Shah, T. Whitehouse, and C. A. Mayhew, "Volatile biomarkers in breath associated with liver cirrhosis—comparisons of pre-and post-liver transplant breath samples (2015)," Ebiomedicine 2, 1243-1250

Di Marzo, L., Cree, P., & Barbano, D. M. (2016). Prediction of fat globule particle size in homogenized milk using Fourier transform mid-infrared spectra. *Journal of Dairy Science*, *99*(11), 8549–8560.

Dryahina K, D. Smith, M. Bortlik, N. Machkova, M. Lukas, and P. Spanel, "Pentane and other volatile organic compounds, including carboxylic acids, in the exhaled breath of patients with Crohn's disease and ulcerative colitis," (2018) J. Breath Res. 12, 9

Heinz Fabian, H., Maentele, W., & Kreutz, W. (1981). Infrared Spectroscopy of Proteins Heinz. *Can. J. Spectrosc.Handbook of Vibrational Spectroscopy*, *26*, 119–125.

Faist J, Capasso F, Sivco DL, et al. (1994) Quantum Cascade Laser. *Science,* 264: 553-556.

Ferreira, I. M. P. L. V. O. (2007). Chromatographic separation and quantification of major human milk proteins. *Journal of Liquid Chromatography and Related Technologies*, *30*(4), 499–507.

Gaugg M.T. , D. G. Gomez, C. Barrios-Collado, G. Vidal-de-Miguel, M. Kohler, R. Zenobi, and P. M. L. Sinues, "Expanding metabolite coverage of real-time breath analysis by coupling a universal secondary electrospray ionization source and high resolution mass spectrometry-a pilot study on tobacco smokers," (2016) J. Breath Res. 10, 9

Henderson B., Khodabakhsh A., Metsälä M., Ventrillard I., Schmidt, F.M., Romanini D., Ritchie G.A.D., te Lintel Hekkert S., Briot R., Risby T., Marczin N., Harren F.J.M., Cristescu S.M. (2018),

J. Mandon, M. Högman, P.J.F.M. Merkus, J. van Amsterdam, F.J.M. Harren, S.M. Cristescu, Exhaled NO monitoring by quantum cascade laser: comparison with chemiluminescent and electrochemical sensors, J. Biomed. Opt. 17, 017003 (2012)

Kuligowski, J., Schwaighofer, A., Alcaráz, M. R., Quintás, G., Mayer, H., Vento, M., & Lendl, B. (2017). External cavity-quantum cascade laser (EC-QCL) spectroscopy for protein analysis in bovine milk. *Analytica Chimica Acta*, *963*(June 2016), 99–105.

Laser spectroscopy for breath analysis: towards clinical implementation, Applied Physics B 124:161, doi 10.1007/s00340-018-70

Lund Myhre, C. E., Christensen, D. H., Nicolaisen, F. M., & Nielsen, C. J. (2003). Spectroscopic study of aqueous $H_2 2SO_4$ at different temperatures and compositions: Variations in dissociation and optical properties. *Journal of Physical Chemistry A*, *107*(12), 1979–1991.

M.M.L. Steeghs, S.M. Cristescu, and F.J.M. Harren, The suitability of Tedlar bags for breath sampling in medical diagnostic research. Physiological Measurement, 2007. 28(1): p. 73-84

Mochalski P., H. Wiesenhofer, M. Allers, S. Zimmermann, A. T. Güntner, N. J. Pineau, W. Lederer, A. Agapiou, C. A. Mayhew, and V. Ruzsanyi, "Monitoring of selected skin- and breath-borne volatile organic compounds emitted from the human body using gas chromatography ion mobility spectrometry (GC-IMS)," (2018) Journal of Chromatography B 1076, 29-34

Montemurro, M., Schwaighofer, A., Schmidt, A., Culzoni, M. J., Mayer, H. K., & Lendl, B. (2019). *proteins and discrimination of commercial milk*, *Analyst*, 2019 (144), 5571–5579.

Neerincx A. H., Mandon J., van Ingen J., Arslanov D. D., Mouton J. W., Harren F. J. M., … Cristescu S. M. (2015). Real-time monitoring of hydrogen cyanide (HCN) and ammonia (NH3) emitted by Pseudomonas aeruginosa. Journal of Breath Research, 9(2), 027102. doi:10.1088/1752-7155/9/2/027102

Phospahte in Urine. (24. September 2019) accessed on 24. september 2019 from Medlineplus: https://medlineplus.gov/lab-tests/phosphate-in-urine/].

Picciano, M. F. (2001). *NUTRIENT COMPOSITION OF*Nutriant composition of human milk. *Pediatr Clin North Am. 48*(1), 53–67.

Putnam, D. (1971). Composition and Concentrative AdministrationProperties of Human Milk. Security, (July).NASA Contractor Report.

Rose, C., Parker, A., Jefferson, B., & Cartmell, E. (2015). The characterization of feces and urine: A review of the literature to inform advanced treatment technology. *Critical Reviews in Environmental Science and Technology*, *45*(17), 1827–1879.

Schmidt, F. M., Metsälä, M., Vaittinen, O., & Halonen, L. (2011). Background levels and diurnal variations of hydrogen cyanide in breath and emitted from skin. Journal of Breath Research, 5(4), 046004. doi:10.1088/1752-7155/5/4/046004

Schwaighofer, A., Kuligowski, J., Quintás, G., Mayer, H. K., & Lendl, B. (2018). Fast quanti fi cation of bovine milk proteins employing external cavity-quantum cascade laser spectroscopy. *Food Chemistry*, *252*(September 2017), 22–27.

Schwaighofer, A., Montemurro, M., Freitag, S., Kristament, C., Culzoni, J., & Lendl, B. (2018*).* Beyond Fourier Transform Infrared Spectroscopy: External Cavity Quantum Cascade Laser-Based Mid-infrared Transmission Spectroscopy of Proteins in the Amide I and Amide II Region. *Anal. Chem,* 90,11,7072.7079.

The importance of methane breath testing: a review J. Breath Res. 7 024001. doi:10.1088/1752-7155/7/2/024001

Velonà T, Abbiati L, Beretta B, et al. (1999) Protein Profiles in Breast Milk from Mothers Delivering Term and Preterm Babies. Pediatric Research, 45: 658.

Vonach, R. , Lendl, B. (1997). Modulation of the pH in the Determination of Phosphate. The Analyst, .122, 525-530

Weida, M. J., & Yee, B. (2011). Quantum cascade laser-based replacement for FTIR microscopy. Imaging, Manipulation, and Analysis of Biomolecules, Cells, and Tissues IX, 7902, 79021C.